# Oleoyl serine, an endogenous *N*-acyl amide, modulates bone remodeling and mass

Reem Smoum[a,b,1], Arik Bar[a,1], Bo Tan[c,1], Garry Milman[b], Malka Attar-Namdar[a], Orr Ofek[a], Jordyn M. Stuart[c], Alon Bajayo[a], Joseph Tam[a], Vardit Kram[a], David O'Dell[c], Michael J. Walker[c], Heather B. Bradshaw[c,2], Itai Bab[a,2,3], and Raphael Mechoulam[b,2]

[a]Bone Laboratory and [b]Institute of Drug Research, Hebrew University of Jerusalem, Jerusalem 91120, Israel; and [c]Indiana University Program in Neuroscience, Indiana University, Bloomington, IN 47405

Edited* by John T. Potts, Massachusetts General Hospital, Charlestown, MA, and approved September 8, 2010 (received for review October 28, 2009)

**Bone mass is determined by a continuous remodeling process, whereby the mineralized matrix is being removed by osteoclasts and subsequently replaced with newly formed bone tissue produced by osteoblasts. Here we report the presence of endogenous amides of long-chain fatty acids with amino acids or with ethanolamine (*N*-acyl amides) in mouse bone. Of these compounds, *N*-oleoyl-L-serine (OS) had the highest activity in an osteoblast proliferation assay. In these cells, OS triggers a Gi-protein-coupled receptor and Erk1/2. It also mitigates osteoclast number by promoting osteoclast apoptosis through the inhibition of Erk1/2 phosphorylation and receptor activator of nuclear-κB ligand (RANKL) expression in bone marrow stromal cells and osteoblasts. In intact mice, OS moderately increases bone volume density mainly by inhibiting bone resorption. However, in a mouse ovariectomy (OVX) model for osteoporosis, OS effectively rescues bone loss by increasing bone formation and markedly restraining bone resorption. The differential effect of exogenous OS in the OVX vs. intact animals is apparently a result of an OVX-induced decrease in skeletal OS levels. These data show that OS is a previously unexplored lipid regulator of bone remodeling. It represents a lead to antiosteoporotic drug discovery, advantageous to currently available therapies, which are essentially either proformative or antiresorptive.**

fatty acyl amides

In mammals, including humans, bone mass is determined by an unremitting remodeling process whereby the mineralized matrix is continuously removed by osteoclasts and subsequently replaced with newly formed bone tissue produced by osteoblasts. This process is regulated by autocrine/paracrine factors, such as receptor activator of nuclear-κB ligand (RANKL), osteoprotegerin (OPG), bone morphogenetic proteins, and Wnt, as well as circulating hormones (e.g., sex steroids, parathyroid hormone) and brain-derived signals (e.g., sympathetic, pituitary) (1–3). Imbalanced bone remodeling leads to skeletal pathologies, mainly osteoporosis, the most common degenerative disorder in affluent societies, which results from a net increase in bone resorption (4). Identification of endogenous constituents, which regulate bone remodeling and skeletal mass, contributes to the elucidation of the mechanisms involved in this process and offers promise for developing novel antiosteoporotic pharmacotherapy.

Amides of long-chain fatty acids with amino acids or with ethanolamine (*N*-acyl amides) represent a major group of endogenous lipids. In mammalian tissues they have numerous physiological functions. For example, anandamide (arachidonoyl ethanolamide) is the first identified endogenous psychoactive ligand of cannabinoid receptors (5); arachidonoyl serine is an endogenous vasodilator, which does not bind to the cannabinoid receptors (6); and oleoyl ethanolamide is an endogenous structural analog to anandamide that regulates food intake through the activation of GPR 119 (7, 8). The well-established biosynthetic tendency to follow existing pathways for the formation of a variety of chemically related natural products prompted us to assess whether the oleic acid amide of serine (oleoyl serine), the fourth and so far missing member of this quartet of compounds (Fig. S1), is also an endogenous ligand. In view of the recent discovery of the skeletal endocannabinoid system (9–11), including the presence in bone of anandamide (12), we focused our assessment on the skeleton. Indeed, partial profiling of fatty acyl amides in trabecular bone revealed the presence of *N*-oleoyl-L-serine (OS), alongside several other molecular entities, at biologically significant levels. Some of these fatty acyl amides stimulate osteoblast proliferation in an in vitro screening assay. Of these, OS showed the highest efficacy. Hence, we further characterized the metabolic activity of OS in bone, including its presence and activity in bone cell systems and normal and osteopenic bone tissue.

## Results

**OS Occurs Naturally in Bone.** To screen for *N*-acyl amides in trabecular bone, we applied a targeted lipidomic strategy to a methanol lipid extract of distal femoral and proximal tibial metaphyses. This strategy has been developed for identifying and quantifying such molecular entities in tissue extracts at high efficiency and sensitivity (13, 14). This screening confirmed the presence of several known compounds, such as anandamide and oleoyl ethanolamide, as well as a previously unexplored constituent, OS (Figs. 1*A* and 2). The structure of OS was elucidated in the lipid extract by chromatographic and structural matching on nanoHPLC/quadrupole time-of-flight (Q-TOF) instrumentation. The D- and L-enantiomers of OS were synthesized according to a standard method for preparing *N*-acyl amino acids (Fig. S2) (15) and used as reference materials for the identification of OS in mammalian tissues. The Q-TOF mass spectrum of the putative OS from bone matched well with that of synthetic OS (Fig. 2 *A* and *B*). The mass errors and putative structures for the predominant molecular species in the spectrum are listed in Table S1. Each predominant mass in the product ion spectrum matched with the mass of an expected structure of OS within ~10 ppm mass errors for the majority of fragments (Fig. 2 *A* and *B* and Table S1). As assessed by matching retention times, the chromatographic behavior of the $368[H^-]/74[H^-]$ mass/charge parent-daughter pair in the tissue extract was the same as that of synthetic OS (Fig. 2 *C*–*E*).

The stereochemistry of the endogenous OS was established by comparing its elution time with that of the synthetic L- and D-enantiomers using chiral HPLC. OS from a partially purified extract and the synthetic L-enantiomer eluted at 46 min; the

Author contributions: M.J.W., H.B.B., I.B., and R.M. designed research; R.S., A. Bar, B.T., G.M., M.A.-N., O.O., J.M.S., A. Bajayo, J.T., V.K., and D.O. performed research; R.S., H.B.B., and I.B. analyzed data; and R.S., H.B.B., I.B., and R.M. wrote the paper.

The authors declare no conflict of interest.

*This Direct Submission article had a prearranged editor.

[1]R.S., A. Bar, and B.T. contributed equally to this work.

[2]H.B.B., I.B., and R.M. contributed equally to this work.

[3]To whom correspondence should be addressed. E-mail: babi@cc.huji.ac.il.

This article contains supporting information online at www.pnas.org/lookup/suppl/doi:10.1073/pnas.0912479107/-/DCSupplemental.

A

| Fatty acyl amides | pmol/g wet bone tissue |
|---|---|
| Oleoyl serine | 3.20±0.25 |
| Arachidonoyl ethanolamide | 0.25±0.008 |
| Oleoyl ethanolamide | 13.7±0.95 |
| Stearoyl ethanolamide | 18.3±1.43 |

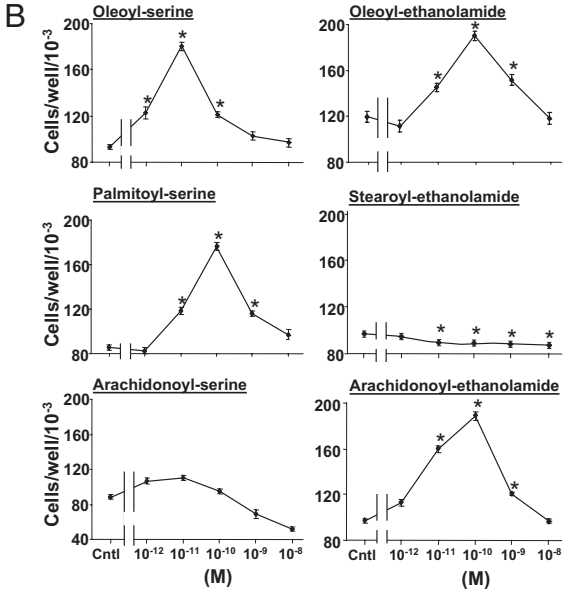


**Fig. 1.** *N*-acyl amides in bone. (*A*) Partial profile of *N*-acyl amides content in metaphyseal extracts of 12-wk-old female mice. Data are mean ± SE obtained in seven mice. (*B*) Proliferative activity of synthetic *N*-acyl amides in MC3T3 E1 osteoblastic cells. Cntl, *N*-acyl amides-free control cultures. Data are mean ± SE obtained in three culture wells per condition. **P* < 0.05, vs. Control.

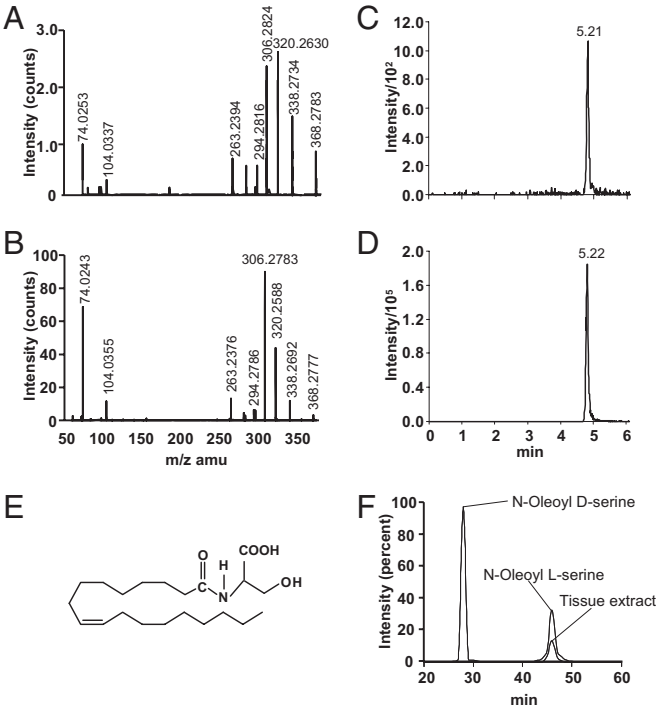


**Fig. 2.** *N*-oleoyl L-serine occurs naturally in bone. (*A* and *B*) Negative product ion spectra of 368.3 of partially purified mouse trabecular bone extract (*A*) and synthetic OS (*B*). (*C* and *D*) Elution profiles of OS from trabecular bone extract (*C*) and synthetic OS (*D*) obtained by reverse-phase HPLC/triple-quadrupole MS. (*E*) Structure of OS. (*F*) Overlay chromatograms of natural and synthetic *N*-oleoyl D-serine (~8 min) and *N*-oleoyl L-serine (~46 min) obtained with chiral HPLC.

synthetic D-enantiomer eluted at 28 min (Fig. 2*F*). Hence, endogenous OS possesses the L rather than the D form.

The OS content in tissues and cell cultures was determined by analysis of lipid extracts on reverse phase HPLC/triple-quadrupole MS. The amount of OS in normal mouse bone was one log higher compared with spleen and one log lower than the brain level. OS was undetectable in plasma, but present in both the MC3T3 E1 osteoblastic cell line and primary newborn-mouse calvarial osteoblasts (Table S2). These findings imply the local production of OS in bone and likely other tissues.

In an osteoblast proliferation screening assay (16), OS and the related compounds presented in Fig. 1*A* stimulated cell number dose-dependently. At higher doses a reversal of the stimulatory effect was noted. Such a biphasic effect has also been reported for cannabinoids in other biological systems (17, 18). The mechanism of this effect is unknown. Of the compounds tested, OS showed the highest efficacy in terms of the dose yielding the peak stimulation and the magnitude of the stimulatory effect (Fig. 1*B*).

**Mitogenic Signaling of OS in Osteoblasts Involves Gi-Protein–ERK1/2 Pathway.** In the osteoblastic cell line MC3T3 E1, OS stimulated DNA synthesis dose-dependently with a peak effect at $10^{-11}$ M ligand concentration (Fig. 3*A*). OS also stimulated the proliferation of primary calvarial osteoblasts (Fig. 3*B*). The OS-induced increase in DNA synthesis was inhibited by pertusis toxin (Fig. 3*C*), indicating that like endocannabinoids (19), OS binds to and activates a Gi-protein coupled receptor (GPCR). Binding analyses for $CB_1$ and $CB_2$ cannabinoid receptors using synaptosomal membranes prepared from rat brains and transfected cells, respectively (20), showed that neither the D nor L form of synthetic OS binds to these receptors up to concentrations of 10 μM. Furthermore, OS stimulated the number of *$CB_2$*-null osteoblasts in a manner similar to that observed in wild-type osteoblasts (Fig. 3*B*). In addition to the absence of $CB_2$, these cells are also deficient of $CB_1$ receptors (11). Hence, these data confirm that the putative OS receptor is a non-cannabinoid GPCR.

Western blot analysis demonstrated that further downstream of the Gi-protein, 5- and 30-min challenges with OS stimulated Erk1/2, but not p38 phosphorylation (Fig. 3*D* and Fig. S3), and that the MEK inhibitor PD98059 lowered the OS proliferative effect (Fig. 3*E*), indicating that Erk1/2 is a critical intracellular mediator of the OS mitogenic activity.

**OS Restricts Osteoclast Life Span.** Reminiscent of the $CB_2$ cannabinoid receptor agonist HU-308 (11), OS also mitigates osteoclastogenesis. The number of tartarate resistant acid phosphatase (TRAP)-positive multinucleated cells in ex vivo bone marrow-derived osteoclastogenic cultures, grown with macrophage colony-stimulating factor (M-CSF) and RANKL (21), was decreased dose-dependently by $10^{-12}$ to $10^{-10}$ M OS (Fig. 4*A*). This decrease reflected enhanced apoptosis at the same OS dose range (Fig. 4 *B–F*). As Erk1/2 are crucial for osteoclast survival (22), we tested the effect of OS on their phosphorylation in a homogenous culture of the osteoclast-like cell line RAW 264.7. Indeed, 5- to 90-min incubation of these cells with $10^{-10}$ M OS inhibited the baseline Erk phosphorylation, in particular Erk2 (Fig. 4*G*), suggesting that Erk activity has an important role in the proapoptotic effect of OS in osteoclasts. In addition to its osteoclastogenic activity, RANKL has been shown to have an important role in osteoclast survival (23). Hence, to assess whether the OS proapoptotic effect is also mediated by the RANKL-RANK axis, we studied the effect of OS on RANKL and OPG expression in stromal cells and osteoblast cultures. In this experiment, OS, already at $10^{-13}$ M, induced more than 90% inhibition of RANKL, but not OPG mRNA levels

MEDICAL SCIENCES

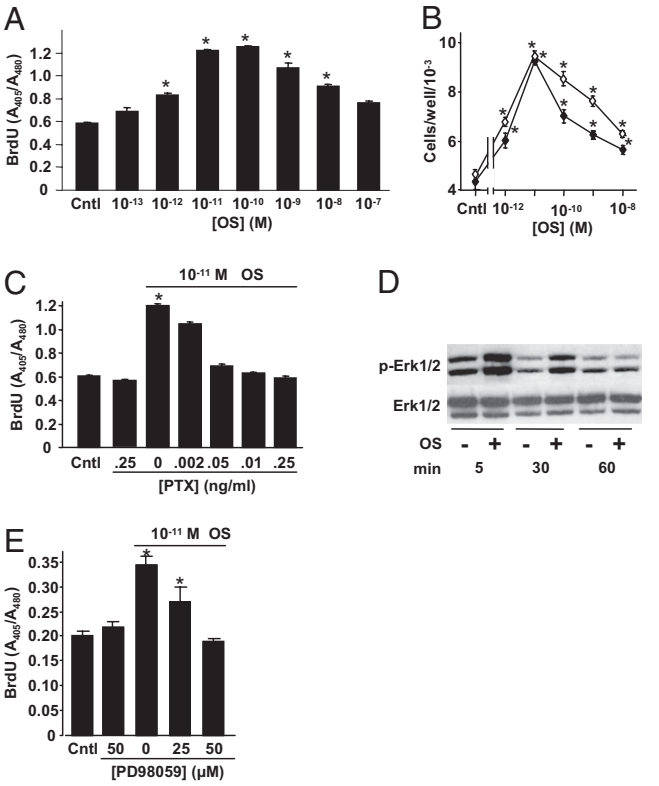


**Fig. 3.** Mitogenic signaling of *N*-oleoyl serine in osteoblasts involves Gi-protein-ERK1/2 pathway. (*A*) DNA synthesis in osteoblastic MC3T3 E1 cells. (*B*) Number of wild-type (●) and $CB_2^{-/-}$ (○) newborn mouse calvarial osteoblast. (*C*) Inhibition of MC3T3 E1 cell DNA synthesis by pertusis toxin (PTX). (*D*) Stimulation of MC3T3 E1 cell Erk1/2 phosphorylation by $10^{-11}$ M OS. (*E*) Inhibition of MC3T3 E1 cell number by MEK inhibitor PD98059. Data are mean ± SE obtained in three culture wells per condition. *$P < 0.05$ vs. Control.

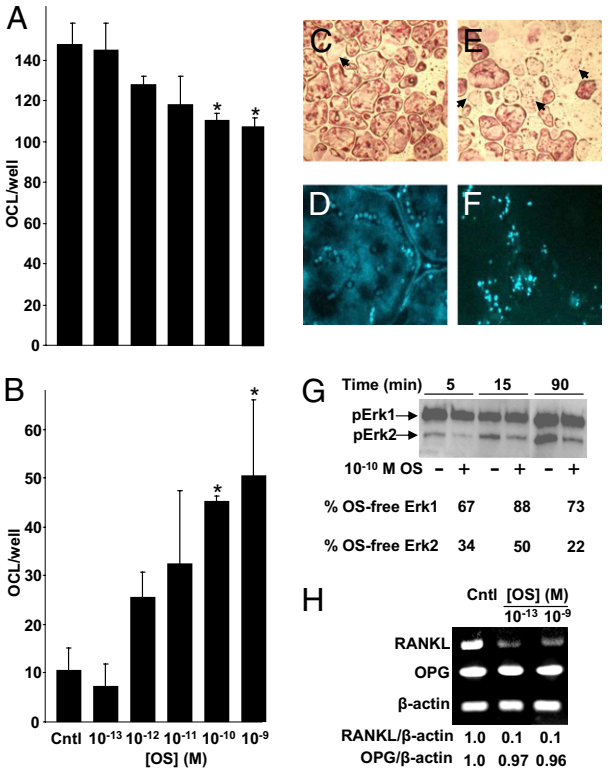


**Fig. 4.** *N*-oleoyl serine inhibits number of intact ostaeoclasts. Osteoclasts were generated from bone marrow monocytes by incubation with M-CSF and RANKL. (*A*) Number of intact osteoclasts. (*B*) Number of apoptotic osteoclasts. (*C* and *D*) OS-free control culture stained with TRAP (*C*) and DAPI (*D*). (*E* and *F*) Cultures challenged with $10^{-10}$ M OS stained with TRAP (*E*) and DAPI (*F*). (*G*) OS inhibition of Erk1/2 phosphorylation in preosteoclast-like RAW 264.7 cells. (*H*) RT-PCR analysis of RANKL and OPG expression in bone marrow-derived primary stromal cells. Quantitative data are mean ± SE obtained in four culture wells per condition. Arrows, apoptotic osteoclasts; *ANOVA, $P < 0.05$ vs. OS-free control (Cntl).

(Fig. 4*H*). These data demonstrate that OS promotes osteoclast apoptosis by cell-autonomous and nonautonomous pathways.

**OS Increases Trabecular Bone Mass in Intact Mice.** Because of the high efficacy of OS in the osteoblast and osteoclast cultures, we further studied the in vivo skeletal activity of exogenously administered OS in intact mice. The mice were treated daily with 5 mg/kg OS given i.p for 6 wk, using ethanol/emulphore/saline (EES) vehicle-treated mice as controls. Importantly, we did not notice any adverse effects of the OS or EES administration, such as attenuated appetite or locomotion. The femora and L3 lumbar vertebral bodies were subjected to microcomputed tomographic (μCT) analysis (11). The trabecular bone-volume density (BV/TV) in the distal femoral metaphysis of the OS treated animals was ∼27% higher compared with vehicle treated mice (Fig. 5 *A* and *B*), mainly secondary to an increase in the trabecular number (Tb.N) rather than trabecular thickness (Tb.Th) (Fig. 5 *C* and *D*). Notably, OS almost doubled the trabecular connectivity (Conn.D) (Fig. 5*E*). OS did not affect the vertebral bone structure (Table S3). To further assess the OS effect on bone remodeling, we determined its effects on the respective bone formation and resorption markers osteocalcin and TRAP5b (24, 25). Although the osteocalcin levels remained unchanged (Fig. 5*F*), immunoreactive TRAP5b showed an ∼7% decrease in the OS-treated mice (Fig. 5*G*). Because part of the treatment period overlapped the phase of bone mass accrual (26), these data suggest that in the intact skeleton OS enhances bone mass and architecture predominantly by inhibiting bone resorption. OS differentially targeted the trabecular bone, as cortical bone parameters were unaffected by OS (Table S4).

**OS Rescues Ovariectomy-Induced Bone Loss.** As OS increases the trabecular bone mass in intact mice, it was of great interest to test its involvement in ovariectomy (OVX)-induced bone loss, an established mouse model for osteoporosis. Sexually mature mice were OVX, or sham-OVX, and left untreated for 6 wk to allow for the occurrence of bone loss and establishment of a new bone-remodeling balance (27). Then, daily i.p. administration of 5 mg/kg OS was initiated in one group of OVX mice. Another group of OVX animals received only the EES solvent. All animals were subjected to a combined μCT and histomorphometric skeletal analysis (11), as well as determination of serum markers of bone remodeling 6 wk after the onset of OS treatment. As in the case of intact mice, the OS or EES treatment was not associated with any adverse effects. The BV/TV in the femora and vertebrae of the vehicle-treated OVX animals was more than 50 and 35%, respectively, lower compared with Sham-OVX mice (Fig. 6 *A* and *B* and Fig. S4 *A* and *B*) primarily because of a decrease in Tb.N (Fig. 6*C* and Fig. S4*C*). OS rescued more than half of the OVX-induced bone loss (Fig. 6*B* and Fig. S4*B*). In the distal femur of the OVX animals, the OS-stimulated increase in BV/TV occurred mainly by enhancing the Tb.Th (Fig. 6*D*). In the vertebral bodies, both the Tb.N and Tb.Th seem to have contributed to the increased BV/TV, although these increases did not reach statistical significance (Fig. S4 *B–D*). Importantly, the connectivity density in the vertebral bodies was also significantly rescued by OS (Fig. S4*E*). Consistent with the cell-culture data, the rescue of OVX-induced bone loss suggests that in addition to its substantial antiresorptive activity (Figs. 5*G*, 6 *H* and *I*), OS

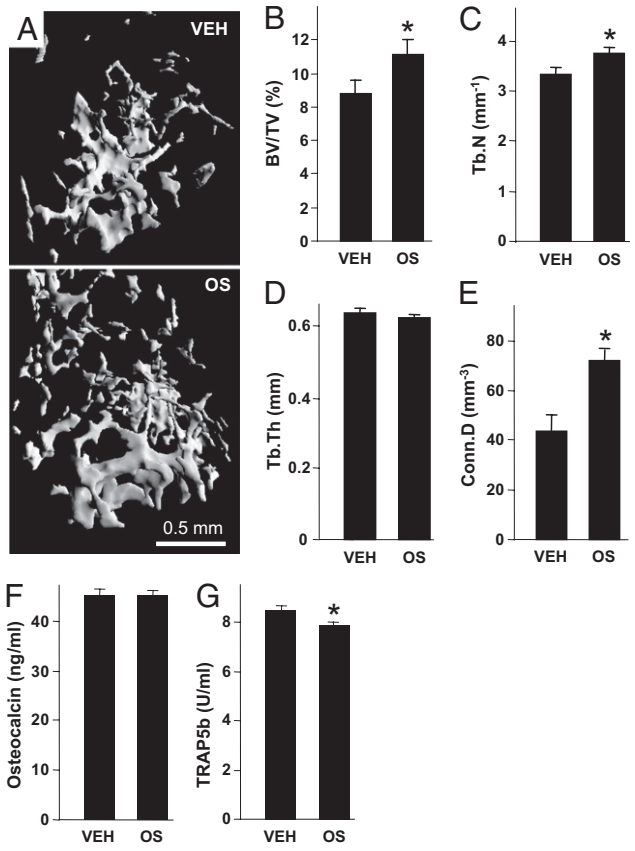


**Fig. 5.** OS increases bone mass in intact mice. (*A*) Femoral metaphyses from mice with median BV/TV. (*B*) Trabecular bone volume density (BV/TV). (*C*) Trabecular number (Tb.N). (*D*) Trabecular thickness (Tb.Th). (*E*) Connectivity density (Conn.D). (*F*) Serum osteoclacin. (*G*) Serum TRAP5b. OS, synthetic *N*-oleoyl L-serine. Data are mean ± SE obtained in 8–12 mice per condition. *Versus VEH; $P < 0.05$.

has a skeletal anabolic activity portrayed here as OS-induced increases in mineral appositional rate (Fig. 6*E*), bone formation rate (Fig. 6*F*), and the serum bone-formation marker osteocalcin (Fig. 6*G*). As OS stimulation of bone formation was not evident in the intact mice (Fig. 5*F*), we speculated that the endogenous OS level is gonadal hormone-dependent. Indeed, determination of the OS levels in the distal femoral metaphysis of a subset of Sham-OVX and OVX mice show an ~35% OVX-induced decrease (Fig. 6*J*). Taken together, the reduced OS level in the OVX animals and the stimulation of bone formation by exogenous OS in the OVX but not intact mice suggest that the physiologic OS level is sufficiently high for maximal OS stimulation of osteoblastic activity. The stimulation of bone formation is primarily attributable to an increase in osteoblast number (Fig. 3*B*), rather than osteoblast activity, as OS did not affect differentiated osteoblast functions, such as alkaline phosphatase activity and matrix mineralization. The rescue of OVX-induced bone loss by OS was selective for the trabecular bone compartment. As in the case of intact mice, in the OVX mice the cortical paramenters were unaffected by the OS administration (Table S5).

## Discussion

We show here the occurrence in trabecular bone of several *N*-acyl amides capable of regulating osteoblast activity. Knowledge on the role of fatty acid ligands and their derivatives in the control of skeletal remodeling and bone mass is scarce. Arguably, our understanding of lipid signaling in cell-to-cell communication in bone is comparable to that of skeletal protein research three to four decades ago. Still, the few compounds studied, such as prostaglandins and endocannabinoids, are among the most potent of these regulators (28, 12).

Of the compounds screened in this study, OS shows the highest efficacy, with a peak effect at $10^{-11}$ M concentration. In view of its high potency, OS was selected as the focus of this study, considering both basic biological processes as well as the identification of promising targets for antiosteoporotic anabolic therapy.

Our findings suggest that OS is produced locally in bone and likely in other tissues. Long-chain fatty acids are known to be metabolized in vivo into amides (29), and it thus seems plausible that oleic acid may be a precursor to OS. Oleic acid is abundantly present in the blood and tissues. It is endogenously biosynthesized from stearic acid (30) or provided exogenously, mainly in olive oil (31). Interestingly, the incidence of osteoporosis is lower in Greece, a fact attributed to the high olive oil consumption in this country (32). Furthermore, *N*-acyl phosphatidylserines have been found (33), which can serve as OS precursors. Whether these or still other biosynthetic pathways are involved in OS production remains to be established.

In osteoblasts the OS activity involves regulation of Erk phosphorylation by a Gi-protein. We have previously reported in these cells that prolonged Gi-protein activation of Erk1/2, beyond 30 min leads to transcriptional activation of Mapkapk2 and Cyclic AMP-responsive element binding (CREB) phosphorylation (16). However, OS failed to increase Mapkapk2 expression (Fig. S5), a finding that may be associated with the relatively short stimulation of Erk1/2 activation, up to 30 min, a time window that may be insufficiently long for the direct induction of transcriptional events. In this regard, the putative OS GPCR differs from the $CB_2$ cannabinoid receptor, also a GPCR (34), which in osteoblasts has a prolonged effect on Erk/12 activation and does stimulate Mapkapk2 mRNA and CREB activity and Cycline D1 mRNA expression (35). Alternatively, the activation of Erk1/2 could stimulate β-catenin expression, thus leading to enhanced osteoblastogenesis (36).

OS stimulated osteoclast apoptosis, thus reducing the number of these cells. Surprisingly, this effect was associated with prolonged inhibition of baseline Erk phosphorylation, in particular Erk2. The differential involvement of Erk2 in apoptotic processes has been reported previously in several cell types, including macrophages, which have the same ontogeny as osteoclasts (37–39). Importantly, the opposing effects of OS on osteoblast and osteoclast Erk indicate that as in the case of the $CB_2$ cannabinoid receptor (11), signaling by the putative OS receptor is cell-type dependent.

In line with the data in the osteoblast and osteoclast cultures, the administration of OS to mice commencing 6 wk after OVX, when the rate of bone loss decreases, leads to some stimulation of bone formation and a substantial inhibition of bone resorption. In contrast, in intact mice there was no effect on bone formation and only a small inhibition of bone resorption. In line with these findings is the rather moderate OS-induced increase in BV/TV in the intact animals (~25%), which was restricted to the femoral site. By comparison, the effect on BV/TV in vehicle- vs. OS-treated OVX mice was ~50 and ~30% higher in the femora and vertebrae, respectively. Furthermore, the OS effect in the intact mice was restricted to distal femoral metaphysis. This differential response to OS is likely because of the marked OVX-induced decrease in endogenous skeletal OS levels. These levels are apparently suboptimal for the regulation of bone remodeling in the estrogen-depleted mice. Hence, these mice are more responsive to the exogenously administered OS. As in the case of endocannabinoids, the regulation of OS levels is likely via biosynthetic and degrading enzymes, such as phospholipases and fatty acid amide hydrolases (40, 41). This putative regulatory system should maintain favorable OS levels, thus preventing adverse outcomes of sub- and supraoptimal concentration, evident in our osteoblast cultures.

It is now recognized that lipid endocannabinoids are produced in the bone microenvironment and regulate bone remodeling and bone mass (12, 42). The identification of OS in the skeleton as

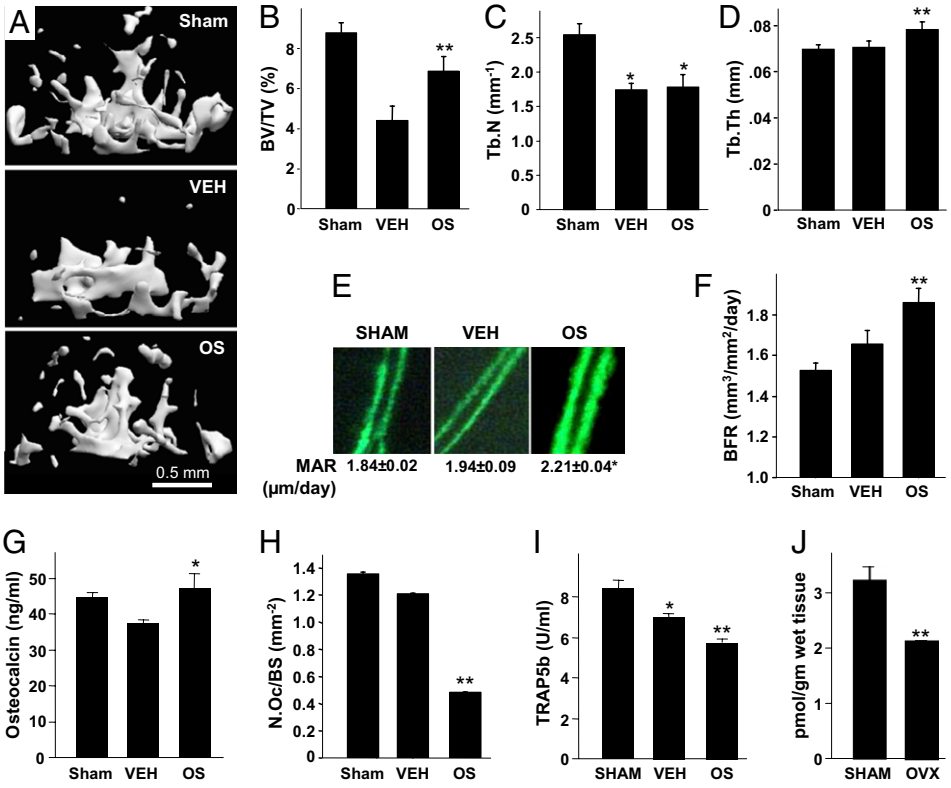


**Fig. 6.** OS regulates bone remodeling and bone mass in distal femoral metaphysis of ovariectomized (OVX) mice. (*A*) Femoral metaphyses from mice with median trabecular bone volume density. (*B*) Trabecular bone volume density (BV/TV). (*C*) Trabecular number (Tb.N). (*D*) Trabecular thickness (Tb.Th). (*E*) Calcein double labels and mineral appositional rate (MAR). (*F*) Bone formation rate (BFR). (*G*) Serum osteocalcin. (*H*) Osteoclast number per trabecular surface area (N.Oc/BS). (*I*) Serum TRAP5b. (*J*) Post-OVX changes in bone OS levels. Data are mean ± SE obtained in six to eight (*A–I*) or five (*I*) mice per condition. *Versus Sham; **vs. VEH, $P < 0.05$.

a potent endogenous lipid regulator of bone remodeling strengthens the evidence for the occurrence of a family of structurally related lipid compounds that control a wide array of physiological functions, not only in the central nervous system, but in peripheral sites as well. The antiresorptive effects of OS in OVX animals are more clearly established than its anabolic effect; however, our data suggest that the latter is also present. Hence, OS represents a lead to novel antiosteoporotic drugs, advantageous to currently available therapies, which are either proformative or antiresorptive.

## Materials and Methods

**Animals.** C57BL/6J mice were used for all experiments involving osteoblast and osteoclast isolation and the in vivo effects of OS in intact and OVX animals. The experimental protocols were approved by the Institutional Animal Care and Use Committees of the Hebrew University of Jerusalem and Indiana University. Mice, 10 wk of age, were subjected to bilateral OVX or sham-OVX. OS was administered intraperitoneally as an ethanol:emulphor:saline (1:1:18) solution. Methanol extracts for OS identification and determination were prepared from the distal femoral metaphysis, whole brain, spleen, and plasma in naive animals and 2 wk after OVX or sham-OVX. Calvarial osteoblasts were obtained form 5-d-old wild-type and $CB_2^{-/-}$ mice (43), kindly provided by Andreas Zimmer (University of Bonn, Bonn, Germany) and bred in the Hebrew University animal facility. Bone marrow-derived monocytes were obtained from the femora and tibiae of 10- to 11-wk-old mice. To assess in vivo the effect of OS on bone formation, newly formed bone was vitally labeled by the fluorochrome calcein (Sigma), and injected intraperitoneally (15 mg/kg) 4 d and 1 d before killing. At death, the femoral bones were separated and preserved, as reported previously (11).

**Synthetic *N*-oleoyl Serine.** The synthesis of OS followed the general pattern for the syntheses of *N*-acyl amino acids (Fig. S1) (15).

**Extraction of *N*-acyl Amides from Tissues for Q-TOF Structural Analysis.** Methods used previously for the isolation and identification of *N*-palmitoyl glycine were employed (13), with the exception that the optimization parameters were based on the retention times and molecular weight of OS. In brief, a modified Folch extraction was performed on the reported tissues. The organic phase was further purified with DEA and C18 solid-phase extraction columns. Matrix samples were separated using a capillary C18 column with nano-flow for analysis by Q-TOF, as previously described (13), with the exception that the product ion scans were made for the OS exact mass of 368.2789 and the Q-TOF ion source for these experiments was from New Objective.

**Quantification of *N*-acyl Amides in Mouse Tissue.** Quantification of OS by HPLC/MS/MS was similar to methods previously described (13). Exceptions to this protocol were that the chromatographic methods were optimized to the OS standard in which multiple reaction monitoring measured the OS 368[$H^-$] parent mass paired to the 104[$H^-$] fragment, and the gradients were optimized to OS peak retention parameters. Quantification of all *N*-acyl ethanolamides was as previously described (44).

**Chiral HPLC Analysis.** To determine chirality of the endogenous OS, modified Folch brain extracts were compared with chiral standards. The chiral HPLC system consisted of Hewlett Packard 1100 binary pumps, an online degasser, Hewlett Packard Interface 35900 E (Agilent) for online graphic representation of UV signals, a manual Cheminert injector (VICI Valco Instruments Co., Inc.), a Shimadzu SPD 10A UV detector, a fraction collector SF-2120 (Advantec MFS Inc.), and a chiral HPLC column (carbamated amylose coated ChiralPak-ADH, 4.6 × 250 mm, 5 μM; Daicel Chemical Industries). The column was loaded with 10-μL samples of either a mixture of equal amounts of synthetic D- and L-oleoyl serine or brain extract. Either sample was dissolved in 3% ethanol/hexane solution containing 0.1% trifluoroacetic acid (the mobile phase). The column was eluted at a flow rate of 1 mL/min with a monitoring wavelength of 205 nm. Compound identity was confirmed by drying the fractions, and reconstituting them in 100 μL methanol and multireaction monitoring analysis with a transition ion pair (368.3–104.3) and the same HPLC-MS/MS system described above for the quantification method.

**Cell Cultures.** MC3T3 E1 osteoblastic cells were maintained as reported previously (45). Newborn mouse calvarial osteoblasts were prepared from 5-d-old mice by successive collagenase digestion (46). The cells were grown to subconfluence in α-MEM supplemented with 10% FCS and then serum-starved for 2 h. Cell counts and BrdU incorporation were determined after additional 48 h incubation in α-MEM supplemented with 0.5% BSA and OS (11). Bone marrow-derived osteoclastogenic cultures were established as reported previously and grown for 4 to 5 d in medium containing M-CSF and RANKL (R&D Systems) (23).

**Western Blot Analysis.** The effect of OS on MAP kinase phosphorylation was studied by immunoblot analysis in the respective MC3T3 E1 and RAW 264.7 osteoblastic and osteoclast-like cells using primary polyclonal antibodies against Erk1/2, phospho-Erk1/2 (Thr202/Tyr204), p38, and phospho-p38 (Thr180/Tyr182) (Cell Signaling Technology, Inc.).

**Effect of OS on Bone Structure and Remodeling.** The skeletal activity of OS was analyzed by a combined μCT/histomorphometric system (11, 47, 48). Briefly, femora and L3 lumbar vertebrae were examined by a μCT system (μCT 40; Scanco Medical AG) at 20-μm resolution in all three spatial dimensions. In the femora, trabecular bone parameters were measured in a metaphyseal segment, extending proximally from the proximal tip of the primary spongiosa to the proximal border of the distal femoral quartile. Cortical bone parameters were determined in a diaphyseal segment extending 1.12 mm distally from the midpoint between the femoral ends. Trabecular bone parameters were also analyzed in L3 bodies. After μCT image acquisition, the femoral specimens were embedded undecalcified in Technovit 9100 (Heraeus Kulzer). Longitudinal sections through the midfrontal plane were left unstained for dynamic histomorphometry based on the vital calcein double labeling. To identify osteoclasts, consecutive sections were stained for TRAP. Parameters were determined according to a standardized nomenclature (49).

**Serum Markers of Bone Remodeling.** Blood from intact and OVX mice was collected retro-orbitally at the time of killing. Serum osteocalcin was determined using a two-site EIA kit (Biomedical Technologies Inc.). Osteoclast-derived TRAP5b was measured in the same specimens using an EIA kit (Immunodiagnostic System Inc.).

**Statistical Analysis.** Differences were analyzed by ANOVA. When significant differences were indicated by ANOVA, group means were compared using the Student-Newman-Keuls test for pairwise comparisons. A *t*-test was used when two samples were compared.

**ACKNOWLEDGMENTS.** This study was supported by United States–Israel Binational Science Foundation Grant 2007013 (to I.B. and H.B.B.) and US National Institute on Drug Abuse Grant 9789 (to R.M.). Purchase of the CT system was supported in part by Grant No. 9007/01 from the Israel Science Foundation (to I.B.).

1. Zaidi M, et al. (2007) Proresorptive actions of FSH and bone loss. *Ann N Y Acad Sci* 1116:376–382.
2. Bodine PV, Komm BS (2006) Wnt signaling and osteoblastogenesis. *Rev Endocr Metab Disord* 7:33–39.
3. Takeda S, Karsenty G (2008) Molecular bases of the sympathetic regulation of bone mass. *Bone* 42:837–840.
4. Weinstein RS, Manolagas SC (2000) Apoptosis and osteoporosis. *Am J Med* 108: 153–164.
5. Devane WA, et al. (1992) Isolation and structure of a brain constituent that binds to the cannabinoid receptor. *Science* 258:1946–1949.
6. Milman G, et al. (2006) *N*-arachidonoyl L-serine, an endocannabinoid-like brain constituent with vasodilatory properties. *Proc Natl Acad Sci USA* 103:2428–2433.
7. Fu J, et al. (2003) Oleylethanolamide regulates feeding and body weight through activation of the nuclear receptor PPAR-alpha. *Nature* 425:90–93.
8. Overton HA, et al. (2006) Deorphanization of a G protein-coupled receptor for oleoylethanolamide and its use in the discovery of small-molecule hypophagic agents. *Cell Metab* 3:167–175.
9. Bab I (2005) *Milestones in Drug Therapy Series*, ed Mechoulam R (Birkhäuser Verlag, Basel), pp 201–206.
10. Idris AI, et al. (2005) Regulation of bone mass, bone loss and osteoclast activity by cannabinoid receptors. *Nat Med* 11:774–779.
11. Ofek O, et al. (2006) Peripheral cannabinoid receptor, CB2, regulates bone mass. *Proc Natl Acad Sci USA* 103:696–701.
12. Bab I, Ofek O, Tam J, Rehnelt J, Zimmer A (2008) Endocannabinoids and the regulation of bone metabolism. *J Neuroendocrinol* 20(Suppl 1):69–74.
13. Rimmerman N, et al. (2008) N-palmitoyl glycine, a novel endogenous lipid that acts as a modulator of calcium influx and nitric oxide production in sensory neurons. *Mol Pharmacol* 74:213–224.
14. Tan B, et al. (2009) Targeted lipidomics approach for endogenous N-acyl amino acids in rat brain tissue. *J Chromatogr B Analyt Technol Biomed Life Sci* 877:2890–2894.
15. Shinitzky M, Haimovitz R (1993) Chiral surfaces in micelles of enantiomeric N-palmitoyl- and N-stearoylserine. *J Am Chem Soc* 115:12545–12549.
16. Miguel SM, Namdar-Attar M, Noh T, Frenkel B, Bab I (2005) ERK1/2-activated de novo Mapkapk2 synthesis is essential for osteogenic growth peptide mitogenic signaling in osteoblastic cells. *J Biol Chem* 280:37495–37502.
17. Sulcova E, Mechoulam R, Fride E (1998) Biphasic effects of anandamide. *Pharmacol Biochem Behav* 59:347–352.
18. Malfait AM, et al. (2000) The nonpsychoactive cannabis constituent cannabidiol is an oral anti-arthritic therapeutic in murine collagen-induced arthritis. *Proc Natl Acad Sci USA* 97:9561–9566.
19. Mackie K (2005) Cannabinoid receptor homo- and heterodimerization. *Life Sci* 77: 1667–1673.
20. Rhee MH, et al. (1997) Cannabinol derivatives: Binding to cannabinoid receptors and inhibition of adenylylcyclase. *J Med Chem* 40:3228–3233.
21. Iqbal J, Sun L, Kumar TR, Blair HC, Zaidi M (2006) Follicle-stimulating hormone stimulates TNF production from immune cells to enhance osteoblast and osteoclast formation. *Proc Natl Acad Sci USA* 103:14925–14930.
22. Miyazaki T, et al. (2000) Reciprocal role of ERK and NF-kappaB pathways in survival and activation of osteoclasts. *J Cell Biol* 148:333–342.
23. Asagiri M, Takayanagi H (2007) The molecular understanding of osteoclast differentiation. *Bone* 40:251–264.
24. Gundberg CM (1998) Biology, physiology and clinical chemistry of osteocalcin. *J Clin Ligand Assay* 21:128–138.
25. Halleen JM, et al. (2000) Tartrate-resistant acid phosphatase 5b: A novel serum marker of bone resorption. *J Bone Miner Res* 15:1337–1345.
26. Bab I, Hajbi-Yonissi C, Gabet Y, Müller R (2007) *Micro-Tomographic Atlas of the Mouse Skeleton* (Springer, New York), pp 198–199.
27. Alexander JM, et al. (2001) Human parathyroid hormone 1-34 reverses bone loss in ovariectomized mice. *J Bone Miner Res* 16:1665–1673.
28. Jee WS, Ma YF (1997) The in vivo anabolic actions of prostaglandins in bone. *Bone* 21: 297–304.
29. Berger A, et al. (2001) Anandamide and diet: Inclusion of dietary arachidonate and docosahexaenoate leads to increased brain levels of the corresponding N-acylethanolamines in piglets. *Proc Natl Acad Sci USA* 98:6402–6406.
30. Ntambi JM, Miyazaki M (2004) Regulation of stearoyl-CoA desaturases and role in metabolism. *Prog Lipid Res* 43:91–104.
31. Boskou D (2000) Olive oil. *World Rev Nutr Diet* 87:56–77.
32. Trichopoulou A, et al. (1997) Energy intake and monounsaturated fat in relation to bone mineral density among women and men in Greece. *Prev Med* 26:395–400.
33. Guan Z, Li S, Smith DC, Shaw WA, Raetz CRH (2007) Identification of *N*-acylphosphatidylserine molecules in eukaryotic cells. *Biochemistry* 46:14500–14513.
34. Munro S, Thomas KL, Abu-Shaar M (1993) Molecular characterization of a peripheral receptor for cannabinoids. *Nature* 365:61–65.
35. Ofek O, et al. (2010) CB2 cannabinoid receptor targets mitogenic Gi protein–cyclin D1 axis in osteoblasts. *J Bone Miner Res*, epub ahead of print.
36. Matsushita T, et al. (2009) Extracellular signal-regulated kinase 1 (ERK1) and ERK2 play essential roles in osteoblast differentiation and in supporting osteoclastogenesis. *Mol Cell Biol* 29:5843–5857.
37. Mohr S, McCormick TS, Lapetina EG (1998) Macrophages resistant to endogenously generated nitric oxide-mediated apoptosis are hypersensitive to exogenously added nitric oxide donors: Dichotomous apoptotic response independent of caspase 3 and reversal by the mitogen-activated protein kinase kinase (MEK) inhibitor PD 098059. *Proc Natl Acad Sci USA* 95:5045–5050.
38. Cho HN, Lee YJ, Cho CK, Lee SJ, Lee YS (2002) Downregulation of ERK2 is essential for the inhibition of radiation-induced cell death in HSP25 overexpressed L929 cells. *Cell Death Differ* 9:448–456.
39. Teitelbaum SL, Abu-Amer Y, Ross FP (1995) Molecular mechanisms of bone resorption. *J Cell Biochem* 59:1–10.
40. Cravatt BF, Lichtman AH (2003) Fatty acid amide hydrolase: An emerging therapeutic target in the endocannabinoid system. *Curr Opin Chem Biol* 7:469–475.
41. Ligresti A, Cascio MG, Di Marzo V (2005) Endocannabinoid metabolic pathways and enzymes. *Curr Drug Targets CNS Neurol Disord* 4:615–623.
42. Tam J, et al. (2008) The cannabinoid CB1 receptor regulates bone formation by modulating adrenergic signaling. *FASEB J* 22:285–294.
43. Buckley NE, et al. (2000) Immunomodulation by cannabinoids is absent in mice deficient for the cannabinoid CB(2) receptor. *Eur J Pharmacol* 396:141–149.
44. Rubio M, McHugh D, Fernández-Ruiz J, Bradshaw H, Walker JM (2007) Short-term exposure to alcohol in rats affects brain levels of anandamide, other *N*-acylethanolamines and 2-arachidonoyl-glycerol. *Neurosci Lett* 421:270–274.
45. Gabarin N, et al. (2001) Mitogenic G(i) protein-MAP kinase signaling cascade in MC3T3-E1 osteogenic cells: Activation by C-terminal pentapeptide of osteogenic growth peptide [OGP(10-14)] and attenuation of activation by cAMP. *J Cell Biochem* 81:594–603.
46. Kato M, et al. (2002) *Cbfa1*-independent decrease in osteoblast proliferation, osteopenia, and persistent embryonic eye vascularization in mice deficient in Lrp5, a Wnt coreceptor. *J Cell Biol* 157:303–314.
47. Bajayo A, et al. (2005) Central IL-1 receptor signaling regulates bone growth and mass. *Proc Natl Acad Sci USA* 102:12956–12961.
48. Yirmiya R, et al. (2006) Depression induces bone loss through stimulation of the sympathetic nervous system. *Proc Natl Acad Sci USA* 103:16876–16881.
49. Parfitt AM, et al.; Report of the ASBMR Histomorphometry Nomenclature Committee (1987) Bone histomorphometry: Standardization of nomenclature, symbols, and units. *J Bone Miner Res* 2:595–610.